Transcriptomes of germinal zones of human and mouse fetal neocortex suggest a role of extracellular matrix in progenitor self-renewal

Simone A. Fietz[a], Robert Lachmann[b,1], Holger Brandl[a,1], Martin Kircher[c], Nikolay Samusik[a], Roland Schröder[c], Naharajan Lakshmanaperumal[a], Ian Henry[a], Johannes Vogt[d,2], Axel Riehn[b], Wolfgang Distler[b], Robert Nitsch[d,2], Wolfgang Enard[c], Svante Pääbo[c,3], and Wieland B. Huttner[a,3]

[a]Max Planck Institute of Molecular Cell Biology and Genetics, 01307 Dresden, Germany; [b]Klinik und Poliklinik für Frauenheilkunde und Geburtshilfe, Universitätsklinikum Carl Gustav Carus, Technische Universität Dresden, 01307 Dresden, Germany; [c]Department of Evolutionary Genetics, Max Planck Institute for Evolutionary Anthropology, 04103 Leipzig, Germany; and [d]Center for Anatomy, Institute of Cell Biology and Neurobiology, Charité, 10117 Berlin, Germany

Contributed by Svante Pääbo, June 8, 2012 (sent for review May 7, 2012)

The expansion of the neocortex during mammalian brain evolution results primarily from an increase in neural progenitor cell divisions in its two principal germinal zones during development, the ventricular zone (VZ) and the subventricular zone (SVZ). Using mRNA sequencing, we analyzed the transcriptomes of fetal human and embryonic mouse VZ, SVZ, and cortical plate. In mouse, the transcriptome of the SVZ was more similar to that of the cortical plate than that of the VZ, whereas in human the opposite was the case, with the inner and outer SVZ being highly related to each other despite their cytoarchitectonic differences. We describe sets of genes that are up- or down-regulated in each germinal zone. These data suggest that cell adhesion and cell–extracellular matrix interactions promote the proliferation and self-renewal of neural progenitors in the developing human neocortex. Notably, relevant extracellular matrix-associated genes include distinct sets of collagens, laminins, proteoglycans, and integrins, along with specific sets of growth factors and morphogens. Our data establish a basis for identifying novel cell-type markers and open up avenues to unravel the molecular basis of neocortex expansion during evolution.

cerebral cortex | neural stem cells | neurogenesis

Neocortex expansion is a hallmark of mammalian brain evolution. With regard to neuron number, a major cause of this expansion is the increase in the population size of neural stem and progenitor cells (NSPCs) and the number of divisions that each of the various NSPC types undergoes during cortical development (1–4). Two principal classes of these cells can be distinguished based on the location of their mitosis: (*i*) apical progenitors (APs), which undergo mitosis at the luminal surface of the ventricular zone (VZ); and (*ii*) basal progenitors (BPs), which undergo mitosis at an abventricular location, typically in the subventricular zone (SVZ) (2, 5, 6). Neurons born from AP and BP cell divisions migrate radially and settle at the basal (pial) side of the developing cortical wall to form the cortical plate (CP).

Both APs and BPs comprise several types of NSPCs that differ in key cell biological features (e.g., cell polarity, cell processes, cell-to-cell junctions, nuclear migration) and in the principal modes of cell division (symmetric proliferative vs. asymmetric self-renewing vs. symmetric or asymmetric consumptive) (2, 5–10). APs comprise neuroepithelial cells, which transform into apical radial glial cells (aRGCs) at the onset of neurogenesis (11), and short neural precursors (12). BPs include basal (or outer) radial glial cells (bRGCs), transit amplifying progenitors (TAPs), and intermediate progenitor cells (IPCs) (2, 3, 13).

The evolutionary expansion of the neocortex is associated with an increase in the thickness of the SVZ, which develops into two cytoarchitecturally distinct zones, an inner SVZ (ISVZ) and an outer SVZ (OSVZ) (1–4, 14, 15). The evolutionary increase in the SVZ is accompanied by a change in the proportion of BP subtypes. For example, in the mouse SVZ (mSVZ), ~90% of the BPs are IPCs, which undergo one terminal round of cell division, and bRGCs and TAPs, which can undergo multiple rounds of cell division, constitute a very minor fraction (13, 16–21). In striking contrast, in the human SVZ (hSVZ), about half of the BPs are bRGCs, and TAPs appear to outnumber IPCs (22–24). To gain insight into the molecular mechanisms underlying the differences in the germinal zones (GZs) of the developing neocortex, and in the NSPCs contained therein, we analyzed the transcriptomes of the VZ, ISVZ, OSVZ, and CP of the human fetal neocortex, and of the VZ, SVZ, and CP of the mouse embryonic neocortex.

Results and Discussion

RNA-Seq of Fetal Human and Embryonic Mouse Cortical Zones. The GZs of the developing neocortex are heterogeneous in terms of the NSPC subpopulations they contain (2, 3). However, as molecular markers applicable for the isolation of cortical NSPC subpopulations are at best partly known, we decided to obtain RNA separately from the various cortical zones. Specifically, we isolated total RNA from the VZ, ISVZ, OSVZ, and CP of six 13–16 wk postconception (wpc) human fetuses and from the VZ, SVZ, and CP of five embryonic day (E) 14.5 mouse embryos (Fig. 1*A* and Fig. S1*A*), using laser-capture microdissection of Nissl-stained cryosections of dorsolateral telencephalon (Fig. S1*A*). Similar experimental approaches have successfully been applied previously in mouse but not in humans (25, 26). Analysis of the RNA quality revealed an RNA integrity number of 8.5–9.5 for all samples (Fig. S1*B*). Poly(A)$^+$ RNA was used as template for the preparation of 24 human and 15 mouse cDNA libraries (Fig. S1*C*), which were then subjected to single-end 76-bp RNA-Seq (Fig. S1*D*). Gene-expression levels were quantified as fragments per kilobase of exon per million fragments mapped (FPKM). Relative expression levels across GZs for eight selected human genes as revealed by RNA-Seq were generally

Author contributions: S.A.F., W.E., S.P., and W.B.H. designed research; S.A.F. performed research; R.L., J.V., A.R., W.D., and R.N. provided fetal human tissue; R.S. assisted in laser-capture microdissection; S.A.F., H.B., M.K., N.S., N.L., and I.H. analyzed data; and S.A.F., W.E., S.P., and W.B.H. wrote the paper.

The authors declare no conflict of interest.

Freely available online through the PNAS open access option.

Data deposition: The data reported in this paper have been deposited in the Gene Expression Omnibus (GEO) database, www.ncbi.nlm.nih.gov/geo (accession no. GSE38805).

[1]R.L. and H.B. contributed equally to this work.

[2]Present address: Institute for Microscopic Anatomy and Neurobiology, University Medicine Mainz, Johannes Gutenberg University Mainz, 55131 Mainz, Germany.

[3]To whom correspondence may be addressed. E-mail: paabo@eva.mpg.de or huttner@mpi-cbg.de.

This article contains supporting information online at www.pnas.org/lookup/suppl/doi:10.1073/pnas.1209647109/-/DCSupplemental.

www.pnas.org/cgi/doi/10.1073/pnas.1209647109

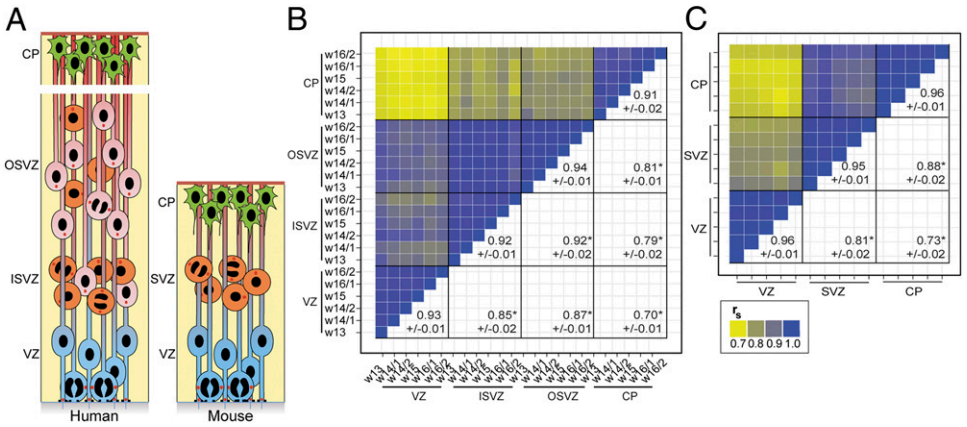

Fig. 1. Correlation analysis of fetal human and embryonic mouse cortical zones. (*A*) Cartoon illustrating the major cell types (APs in blue, BPs in orange and red, neurons in green) in the different GZs and the CP of the developing mouse and human neocortex. (*B* and *C*) Heatmap showing pair-wise correlations of gene expression levels between the indicated zones of the fetal human neocortex at the indicated gestational weeks (*B*, 13–16 wpc) and of the E14.5 mouse neocortex (*C*). Spearman's rank correlation coefficients (r_s) range from 0.7 (yellow) to 1.0 (blue). Numbers in the blank quadrants indicate the mean r_s values ± SD of the zone comparison located mirror-symmetrically to the diagonal line; asterisks indicate zone comparison mean r_s values that show a statistically significant difference to each other ($P < 0.05$).

concordant with those obtained by quantitative PCR of total RNA, thus validating the RNA-Seq data (Fig. S2).

For an initial characterization of the gene-expression patterns in the fetal human cortical zones, we used the FPKM values to calculate pair-wise correlations between the 13–16 wpc samples within a given zone and between the four zones (Fig. 1*B*). The resulting correlation coefficients were used to cluster the various 13–16 wpc zones into a correlation dendrogram (Fig. S3*A*). This analysis revealed that the transcriptomes of the three GZs were more closely related to each other than to the CP, with the ISVZ and OSVZ being most closely related to each other. Remarkably, the OSVZ showed a slightly closer relationship to the VZ than did the ISVZ, despite its larger spatial distance to the VZ. Only little differences were found with regard to the various fetal stages (13–16 wpc). Importantly, the same analysis for E14.5 mouse showed that, in contrast to human, the transcriptome of the SVZ was more closely related to that of the CP than was the VZ (Fig. 1*C* and Fig. S3*B*). This finding is consistent with the notion that in human, all three GZs characteristically contain self-renewing NSPCs, whereas in mouse this holds true only for the VZ.

Expression Patterns of Marker Genes. The various human and mouse NSPCs have previously been characterized with regard to the expression of molecular markers, in most cases using immunohistochemistry (2, 3, 5, 6, 8, 27, 28). We examined the mRNA expression levels of selected markers of APs, BPs, and neurons in the different zones (Fig. S4). The mRNA of the AP marker prominin-1 was predominantly expressed in the hVZ and mVZ (Fig. S4 *B* and *I*). In both species, mRNA levels for Pax6, nestin, and GLAST, known to be expressed by APs and bRGCs (2, 3, 5, 6, 22, 23, 27–29), were highest in the VZ and lowest in the CP. Interestingly, these mRNAs were relatively stronger expressed in hISVZ and hOSVZ than in mSVZ (Fig. S4 *B* and *I*). This finding is consistent with the much higher abundance of bRGCs in hISVZ and hOSVZ than mSVZ (13, 20–23) as revealed, for example, by the greater proportion of $Pax6^+$ nuclei in hSVZ (Fig. S4*E*) than mSVZ (28).

Markers of TAPs/IPCs and of TAP/IPC-generation (Tbr2, neurogenin-2, Svet1, Insm1) were highly expressed in all GZs but only weakly in the hCP and mCP (Fig. S4 *C* and *J*). Remarkably, however, the relative levels of the Tbr2 and neurogenin-2 mRNAs were higher in mVZ than mSVZ (Fig. S4*J*), whereas the opposite has been observed for the Tbr2 protein by immunohistochemistry (27, 28). In contrast, the Tbr2 and neurogenin-2 mRNAs were lower in the hVZ than hISVZ and hOSVZ (Fig. S4*C*), in accordance with Tbr2 immunohistochemistry (Fig. S4*F*). These data are consistent with the notion that in mouse the vast majority of BPs are IPCs, which are generated in the VZ (5, 6, 16–19, 30), whereas in human most $Tbr2^+$ BPs are thought to be generated in the SVZ (2, 3, 22).

mRNA levels of neuronal markers (βIII-tubulin, Tbr1, NeuroD2, NF-M) were highest in the h/mCP, intermediate in the hISVZ/OSVZ and mSVZ, and lowest in the h/mVZ (Fig. S4 *D* and *K*), as observed for Tbr1 protein by immunohistochemistry (Fig. S4*G*). This finding is consistent with the notion that in mouse (17, 19, 31) and human (2, 3), BPs generate substantially more neurons than APs. The similar proportions of neuronal marker mRNAs in the mSVZ and hSVZ indicate that the higher similarity of expression patterns between the VZ and SVZ in human compared with mouse (Fig. 1 and Fig. S3) is not because of a different contribution of neurons, but might indeed reflect the common potential for self-renewal.

Genes Differentially Expressed Between Cortical Zones. We used DESeq (Fig. 2*A*, and Fig. S5 *A* and *C*) to identify sets of genes significantly up- or down-regulated in the human (Fig. 2*B* and Dataset S1) and mouse (Fig. S5*B* and Dataset S1) cortical zones. [Because only the $poly(A)^+$ RNAs had been used as templates for the preparation of the cDNA libraries, we focused our analysis on protein-encoding RNAs.] In line with the high similarity in overall gene expression between hISVZ and hOSVZ (Figs. 1 and 2*A*, and Fig. S3), these two zones had the smallest numbers of differentially expressed genes (Fig. 2*B*, red and orange). Interestingly, the 55 genes up-regulated in hOSVZ relative to hVZ, hISVZ, and hCP, as well as the 20 genes up-regulated in the hOSVZ relative to all other human and mouse zones (Dataset S1), included Olig1 and Sox10, which have been implicated in oligodendrogenesis (32, 33). Moreover, both these gene groups included two highly related but functionally poorly understood genes, KIAA1324 and KIAA1324-like, which showed barely detectable expression in the two mGZs (Dataset S1). These genes are thus potential novel markers for hOSVZ.

To gain insight into the biological processes associated with the large number of genes up- or down-regulated in human CP compared with the VZ, ISVZ, and OSVZ, OSVZ compared with VZ and CP, ISVZ compared with VZ and CP, and VZ compared with ISVZ, OSVZ, and CP (Fig. 2*B*), we used DAVID (34) to cluster the functional gene annotation (FGA) terms significantly overrepresented in these sets of genes (Fig. 2*C* and Dataset S2). The same analysis was performed among the mouse zones (Fig. 3*A* and Dataset S2), hCP vs. mCP, hOSVZ or hISVZ vs. mSVZ, and hVZ vs. mVZ (Fig. 3*B* and Dataset S2). From this comparison, four major findings emerged.

First, the majority (53%) of the five FGA terms most enriched among the genes with higher expression in either the hOSVZ, hISVZ, or hVZ were highly related, or identical, to each other, and concerned cell-to-extracellular matrix (ECM) interaction and the secretory processes underlying both the secretion of ECM constituents and the surface delivery of the corresponding receptors (Fig. 2*C*, *Left*, and Dataset S2). Second, FGA terms associated with ECM interaction and cell adhesion were

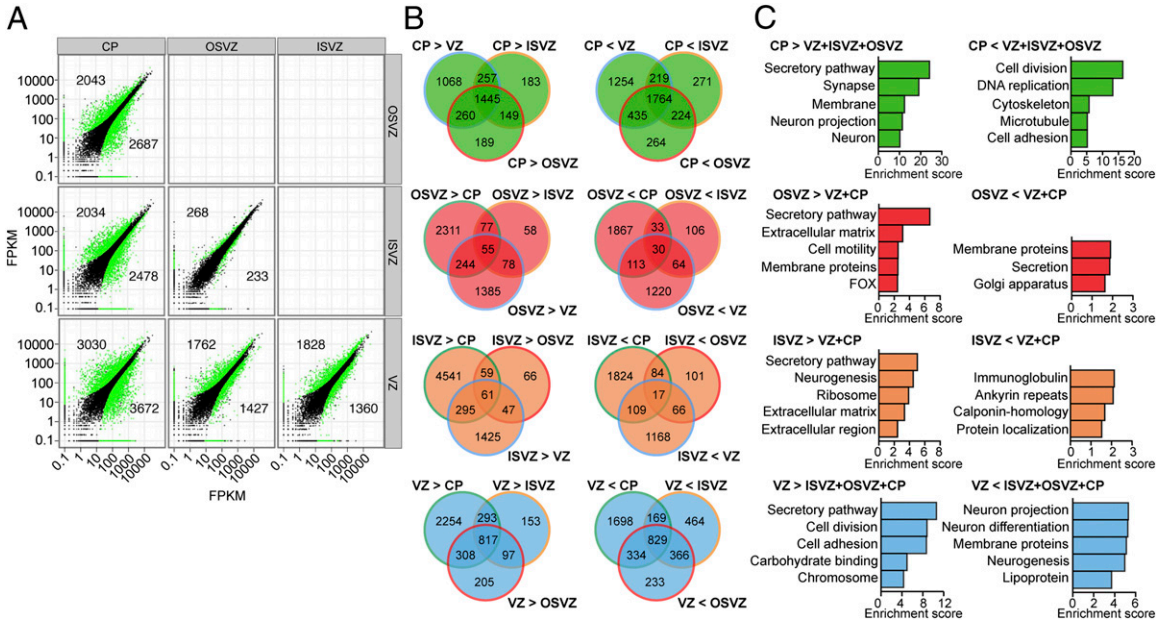

Fig. 2. Differential gene-expression analysis and functional annotation clustering of fetal human cortical zones. (*A*) DESeq scatter plot showing pair-wise comparisons of gene expression between the indicated zones of the 14–16 wpc human neocortex. Each dot represents the mean (five fetuses) expression level for a given gene, with differentially expressed genes (false-discovery rate <0.05) shown in green. Numbers above (below) the diagonal lines refer to the differentially expressed genes up-regulated in the zone indicated on top (on the right). These numbers include the genes expressed in only one of the two zones compared (green dots on vertical and horizontal 0.1 lines). For the corresponding analysis of genes differentially expressed in mouse zones and between human and mouse zones see Fig. S5. (*B*) Venn diagrams showing the numbers of differentially expressed genes (see *A*) that are up-regulated (*Left*, >) and down-regulated (*Right*, <) in a given zone compared with the other zones of the 14–16 wpc human neocortex. (*C*) Differentially expressed genes (see *A*) that are up-regulated (*Left*, >) and down-regulated (*Right*, <) in a given zone compared with the other zones indicated of the 14–16 wpc human neocortex were analyzed for significantly enriched FGA terms which were clustered, using DAVID. The five clusters with the highest enrichment scores are shown. Note that for certain FGA terms enriched in the various GZs, the same designation were chosen (e.g., secretory pathway), although the individual genes in these clusters were different.

enriched among the genes with lower expression in the mSVZ (Fig. 3*A*, orange *Right*, and Dataset S2). Third, when comparing mVZ with mSVZ and mCP, FGA terms related to cell division and DNA replication (rather than ECM interactions) were strikingly overrepresented (Fig. 3*A*, blue *Left*, and Dataset S2). Fourth, FGA terms associated with ECM interaction, the secretory process, and cell adhesion constituted the vast majority of terms overrepresented among genes with higher expression in hGZs compared with mGZs (Fig. 3*B*, *Left*, and Dataset S2).

Taken together, these data suggest that NSPCs in hGZs are more dependent on ECM interactions and associated secretory pathways than is the case for mouse. Because the majority of neural NSPCs in the developing human neocortex (APs, bRGCs, and TAPs), in contrast to the majority of mouse BPs, are capable of undergoing self-renewing divisions, ECM interactions may promote the capacity for sustained self-renewal of NSPCs in the hGZs. This notion is consistent with previous observations and concepts (35–38) and with our previous findings concerning bRGC maintenance in ferrets and its dependence on integrin signaling (23).

Cluster Analysis of Genes Related to Cell–ECM Interaction. To obtain further insights into the putative role of the ECM for proliferation and self-renewal of NSPCs, we performed mean-shift clustering of those genes for which the DAVID FGA terms included ECM, extracellular region, ECM–receptor interaction, proteoglycan, and basement membrane (referred to as ECM-associated genes). (See Fig. S6 and *SI Results and Discussion* for the results of mean-shift clustering of all genes.) This analysis yielded nine clusters that differed in the pattern of gene-expression levels across the mouse and human zones (Fig. 4 *A–J*). In five of these clusters (Fig. 4 *B–F*), the median gene expression in the hVZ and mVZ, hISVZ, and hOSVZ was higher than in the other zones; these clusters are therefore referred to as "GZ clusters." These expression patterns indicated that the genes in these clusters included those of relevance for NSPC self-renewal. Inspection of the gene lists of the five GZ clusters yielded the following insights.

One GZ cluster (198 genes) (Fig. 4 *A* and *B* and Dataset S3) contained genes most highly expressed in h/mVZ and to a lesser extent in hISVZ and hOSVZ. Enriched FGA terms included growth factor binding, heparin binding, cell proliferation, basement membrane, and the Notch signaling pathway (Dataset S4). As the expression pattern of this cluster reflected the relative abundance of aRGCs and bRGCs in the hGZs and mGZs, the genes contained therein include candidates for supporting self-renewal of these NSPCs in an autocrine manner.

Three GZ clusters contained ECM-associated genes more highly expressed in the GZs than CP of human but not mouse (Fig. 4 *A*, *C*, *D*, and *F*, and Dataset S3). The first cluster showed a median gene-expression pattern hVZ > hISVZ/hOSVZ (126 genes) (Fig. 4 *A* and *C*), and hence may contain genes that specifically support the self-renewal of human—but not mouse—NSPCs. The second cluster contained ECM-associated genes most highly expressed in the hVZ but not hISVZ and hOSVZ (68 genes) (Fig. 4 *A* and *D*, and Dataset S3). Similarly, a distinct cluster was obtained for the mVZ (79 genes) (Fig. 4 *A* and *E*, and Dataset S3). This finding implies that the ECM-associated genes that would specifically support autocrine self-renewal of aRGCs would be distinct for the hVZ and mVZ. The third hGZ cluster showed a median gene-expression pattern hISVZ = hOSVZ but not hVZ (78 genes) (Fig. 4 *A* and *F*, and Dataset S3). This cluster presumably contains ECM-associated genes involved in hSVZ-specific aspects of NSPC behavior. Strikingly, enriched FGA terms related to regulation of vasoconstriction, blood vessel remodeling, and hormone activity were found in this, but not in the other GZ clusters (Dataset S4).

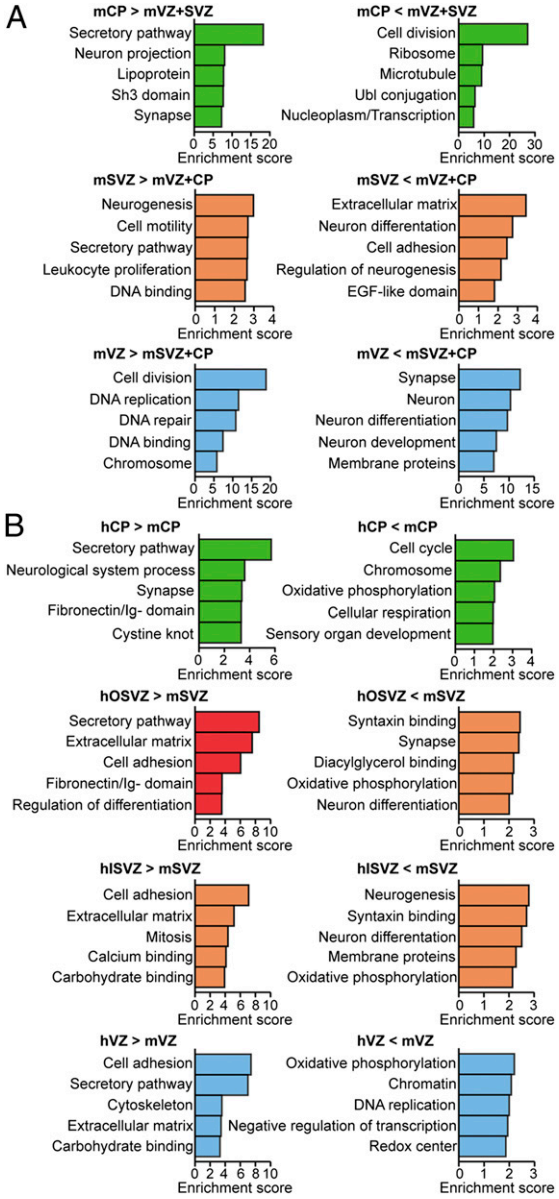

Fig. 3. Functional annotation clustering of genes differentially expressed among mouse cortical zones and between human and mouse cortical zones. Differentially expressed genes identified by DESeq (Fig. S5) that are up-regulated (*Left*, >) and down-regulated (*Right*, <) between the indicated zones of the E14.5 mouse neocortex (*A*) and between the 14–16 wpc human and E14.5 mouse neocortex (*B*) were analyzed for significantly enriched FGA terms, which were clustered, using DAVID. The five clusters with the highest enrichment scores are shown. See note on FGA terms in Fig. 2C.

In addition to the five GZ clusters, we obtained four clusters, referred to as "CP clusters," that contained ECM-associated genes more highly expressed in the hCP and/or mCP than in the hGZs and mVZ (Fig. 4 *G–J* and Dataset S3). These genes are likely not of relevance for NSPC self-renewal. The CP clusters consisted of two with genes most highly expressed in the hCP and mCP [43 genes (Fig. 4*H*), 97 genes (Fig. 4*I* and Dataset S3)], and two containing genes most highly expressed only in hCP (65 genes) (Fig. 4*J* and Dataset S3) or mCP (53 genes) (Fig. 4*G* and Dataset S3). Remarkably, genes more highly expressed in the mSVZ than other GZs were found in one of the CP clusters (Fig. 4*I*) rather than the GZ clusters. The vast majority of the enriched FGA terms in the cluster shown in Fig. 4*I* were related to neuronal maturation processes (Dataset S4), consistent with the notion that such processes occur not only in the CP but presumably also in the mSVZ. Half of the enriched FGA terms in the cluster shown in Fig. 4*H* were related to Golgi-associated processes (Dataset S4), in line with the notion that establishing neuronal function is particularly dependent on the activity of the Golgi complex (39).

When focusing on the classic ECM constituents and receptors among the ECM-associated genes, collagen genes were exclusively present in the GZ clusters (Fig. 4*K* and Dataset S3). Moreover, the vast majority of the laminins (Fig. 4*L* and Dataset S3), proteoglycans (Fig. 4*M* and Dataset S3), and integrins (Fig. 4*N* and Dataset S3) were also found in the GZ clusters. Interestingly, when focusing on individual zones, in human the overwhelming majority of the ECM-associated genes were shared between the GZs, with only a few being specific for either hVZ or hISVZ/OSVZ, and with ECM-associated genes in hCP being clearly distinct (Fig. 4*P*). In contrast, in mouse the ECM-associated genes were shared between the mCP and mSVZ, but were distinct for the mVZ (Fig. 4*P*). These data have significant implications with regard to the site of production of specific ECM constituents in the developing human versus mouse neocortex and their potential role in the differential self-renewal capacity of human versus mouse NSPCs, as is discussed below.

Finally, it is important to emphasize that the majority of growth factors and morphogens included with the ECM-associated genes were found in the GZ clusters rather than the CP clusters (Fig. 4*O* and Dataset S3). This finding points to an interplay between these factors and the ECM/ECM receptors in the signaling that ultimately influences the various types of NSPCs in the developing human and mouse neocortex.

Putative Regulation of ECM-Associated Genes by Transcription Factors. We sought to obtain clues as to the transcription factors (TFs) that may regulate the ECM-associated genes within the nine clusters (Fig. 4 *B–J*). To this end, for each cluster, the promoter regions of the genes contained therein were analyzed for overrepresentation of specific TF binding sites using oPOSSUM (40, 41). The TFs implicated in the various expression patterns of ECM-associated genes across human and mouse cortical zones were then analyzed for their relative abundance in these zones. Only those TFs were considered that showed a significantly ($P < 0.05$) higher expression level in the cortical zones with a median $\log_2$ fold-change >0 (Fig. 4 *B–J*, red columns) compared with those with a median $\log_2$ fold-change <0 (Fig. 4 *B–J*, green columns).

This analysis revealed strikingly different sets of TFs putatively regulating the ECM-related genes in hGZs and mVZ vs. h/mCP and mSVZ (Dataset S5). Remarkably, there was substantial overlap in the TFs between the five GZ clusters, suggesting that highly related transcriptional networks may drive the expression of ECM-associated genes in those h/mGZs that are characterized by a high abundance of self-renewing NSPCs. Interestingly, these candidate TFs included not only some already known to be involved in NSPC self-renewal, such as Sox2, but also transcriptional regulators not previously implicated in this process, such as ZNF143 (Dataset S5).

Conclusions

We provide genome-wide RNA-Seq–based expression data for the distinct GZs of the fetal human neocortex. Recently, similar data have been reported for the mouse (26), extending previous gene-expression studies on embryonic cortical NSPCs using microarray analyses (see e.g., refs. 28 and 42). In contrast, for humans, only different areas of the fetal neocortex, without distinguishing GZs and the CP, have been studied (43). The implications of our data with regard to NSPCs in the developing human versus mouse neocortex and the potential role of the ECM in their self-renewal capacity include the following.

First, despite their cytoarchitectonic differences (14), gene expression in the hISVZ and hOSVZ was found to be very similar. This finding presumably reflects the fact that the various

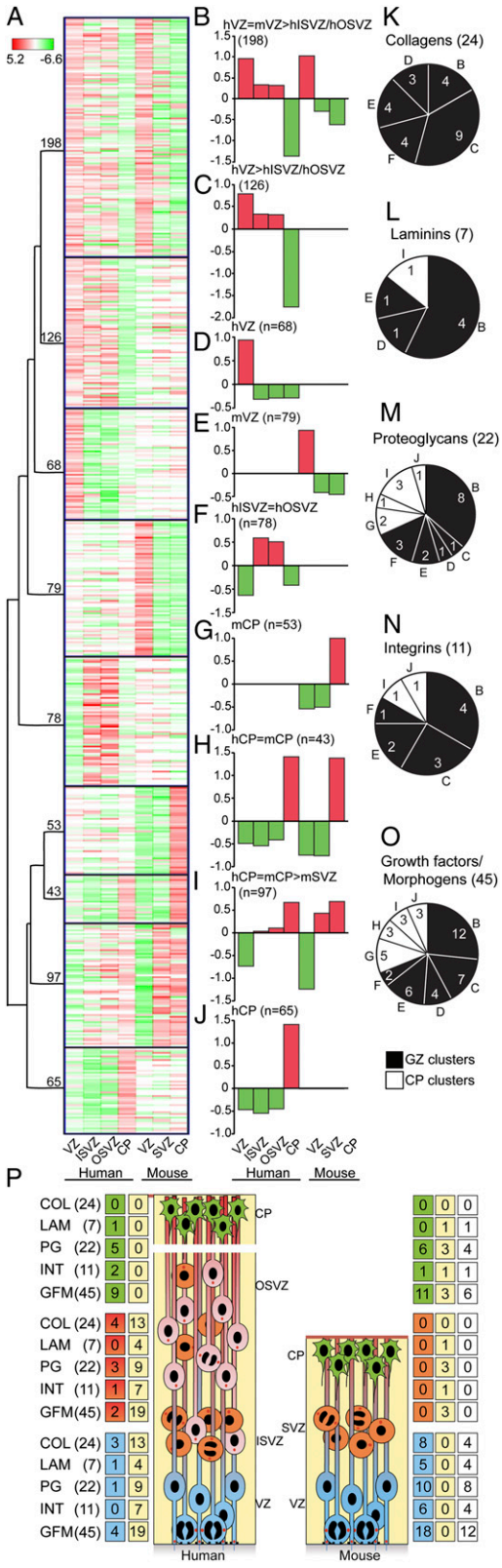

Fig. 4. Mean-shift clustering of genes related to ECM interaction in fetal human and embryonic mouse cortical zones. (*A–J*) Log_2-transformed FPKM fold-changes of ECM-related genes in the 14–16 wpc hVZ, hISVZ, hOSVZ, and hCP (five fetuses) and in the E14.5 mVZ, mSVZ, and mCP (five embryos) relative to the mean expression of each of the genes in all human or mouse zones were subjected to nonhierarchical K-nearest neighbor mean-shift (KNN-MS) cluster analysis, which yielded a total of nine clusters. (*A*) Heat map showing the nine clusters sorted hierarchically using an average-linkage algorithm. Each gene is represented by a single row and each developmental stage by a single column. Fold-changes range from 5.2 (red) to −6.6 (green). (*B–J*) Median log_2 fold-changes in expression of the genes (numbers in parentheses) contained in the nine clusters shown in *A*. (*K–O*) Occurrence of collagens (*K*), laminins (*L*), proteoglycans (*M*), integrins (*N*), and growth factors/morphogens (*O*) in the clusters indicated in *B–J* of the 14–16 wpc human (five fetuses) or E14.5 mouse (five embryos) neocortex. Numbers in parentheses refer to the total number of collagen, laminin, proteoglycan, integrin, or growth factor/morphogen genes expressed in the fetal human and embryonic mouse neocortex; numbers in the pie chart sectors refer to the number of the respective genes expressed in the indicated cluster. Black sectors, GZ clusters; white sectors, CP clusters. (*P*) Summary of the distribution of collagens (COL), laminins (LAM), proteoglycans (PG), integrins (INT), and growth factors/morphogens (GFM) between the various zones of fetal human and embryonic mouse neocortex (APs in blue, BPs in orange and red, neurons in green). Numbers in parentheses, total number of genes in respective class, as indicated in *K–O*; numbers in green/red/blue boxes, number of genes in respective class that are specifically overexpressed (red bars in *B–J*) only in the hCP or mCP (green), hISVZ, and hOSVZ or mSVZ (red), or hVZ or mVZ (blue); numbers in yellow boxes, number of genes in respective class that are overexpressed in more than one human or mouse zone; numbers in white boxes, number of genes in respective class that are overexpressed in both h/mVZ, hISVZ/hOSVZ/mSVZ, or h/mCP.

subtypes of BPs—that is, bRGCs, TAPs, and IPCs—are found in both, hISVZ and hOSVZ, albeit at different relative abundance.

Second, the functional annotations of genes differentially expressed in the various GZs revealed that increased ECM interaction and cell adhesion may underlie the greater self-renewal capacity of NSPCs in hGZs and the mVZ compared with the mSVZ. Potentially relevant ECM-associated genes include distinct sets of collagens, laminins, proteoglycans, and integrins, along with specific growth factors and morphogens. Our findings are in line with previous concepts (35–38) and with the recent findings that (*i*) mouse NSPCs undergoing terminal neurogenic division down-regulate gene products enabling ECM interactions (28), and (*ii*) interference with integrin signaling reduces the abundance of ferret bRGCs (23).

Third, a role of ECM constituents and receptors in NSPC self-renewal during cortical development may contribute to explaining the phenotypes observed in mice and humans carrying mutations in ECM genes. For example, loss of the proteoglycan perlecan results in microcephaly in mouse (44, 45) and human (46). Interestingly, we found that perlecan was more highly expressed in those h/mGZs that are known to be rich in self-renewing NSPCs (Fig. 4*B*). Moreover, the perlecan-containing cluster of ECM-associated genes (Fig. 4*B*) also contained fibulin-4 (EFEMP2), mutations of which also cause microcephaly in human (47).

Fourth, our findings that the three hGZs and the mVZ are major sites of production not only of ECM receptors, but also of ECM constituents, have interesting implications as to the cell biological basis underlying the putative ECM-based promotion of NSPC self-renewal. On the one hand, these cells may contribute, via vesicular transport in their basal processes, to the deposition of ECM constituents at the basal lamina, contact with which likely supports NSPC self-renewal (23). In this context, it is interesting to note that genes, mutations in which result in major basal lamina defects and cortical development disorders, such as fukutin (48), were more highly expressed in those h/mGZs that contain aRGCs and bRGCs (Fig. 4*B*). On the other hand, ECM constituents may also be deposited locally in the GZs themselves, thereby creating a microenvironment conducive for cell proliferation and self-renewal.

In other words, NSPCs in the three hGZs and mVZ, but not the mSVZ, may generate their own niche. In the first of the above scenarios, this niche is linked to the basal side of the developing cortical wall (i.e., the basal lamina at the pial surface). In the second scenario, this niche is generated locally in those

GZs in which the majority of NSPCs can undergo self-renewal. These two scenarios are not mutually exclusive. Moreover, the basal lamina-containing blood vessels that occur throughout the GZs (49–51) may constitute an additional embryonic neural stem cell niche.

Finally, the present catalogs of genes differentially expressed among the various GZs of fetal human and embryonic mouse neocortex will help identify molecular markers for NSPC subtypes, notably BP subtypes, including cell-surface molecules that could be used to isolate NSPC subpopulations. This approach would extend previous microarray studies on NSPC subpopulations isolated from embryonic mouse neocortex (28, 42). Moreover, comparison of gene-expression profiles between the various human and mouse NSPC subtypes may provide clues as to which genes control the number of proliferative and self-renewing divisions, which in turn should lead to insight into the interspecies differences in NSPC behavior during neocortex development that underlie the differences in neocortex expansion among species.

Methods

Fetal human and embryonic mouse cortical zones were obtained by laser-capture microdissection, subjected to RNA-Seq, and analyzed using state-of-the-art methods. Details can be found in *SI Methods*. See Datasets S6 and S7 for further data regarding functional annotations of genes of each cluster using mean-shift clustering.

ACKNOWLEDGMENTS. We thank the sequencing group of the Max Planck Institute for Evolutionary Anthropology, and Jussi Helppi and other members of the animal facility of the Max Planck Institute of Molecular Cell Biology and Genetics for excellent support; Henrike Heyne, Birgit Nickel, and other members of the S.P. group for experimental advice; Dr. Denise Stenzel of the W.B.H. group for discussion; and Vineeth Surendranath of the Max Planck Institute of Molecular Cell Biology and Genetics for helpful comments regarding data analysis. S.A.F. and N.S. were members of the International Max Planck Research School for Molecular Cell Biology and Bioengineering. W.B.H. was supported by grants from the Deutsche Forschungsgemeinschaft (SFB 655, A2; TRR 83, Tp6) and the European Research Council (250197), by the Deutsche Forschungsgemeinschaft-funded Center for Regenerative Therapies Dresden, and by the Fonds der Chemischen Industrie.

1. Rakic P (2009) Evolution of the neocortex: A perspective from developmental biology. *Nat Rev Neurosci* 10:724–735.
2. Fietz SA, Huttner WB (2011) Cortical progenitor expansion, self-renewal and neurogenesis-a polarized perspective. *Curr Opin Neurobiol* 21:23–35.
3. Lui JH, Hansen DV, Kriegstein AR (2011) Development and evolution of the human neocortex. *Cell* 146:18–36.
4. Molnár Z (2011) Evolution of cerebral cortical development. *Brain Behav Evol* 78:94–107.
5. Götz M, Huttner WB (2005) The cell biology of neurogenesis. *Nat Rev Mol Cell Biol* 6: 777–788.
6. Kriegstein A, Alvarez-Buylla A (2009) The glial nature of embryonic and adult neural stem cells. *Annu Rev Neurosci* 32:149–184.
7. Huttner WB, Kosodo Y (2005) Symmetric versus asymmetric cell division during neurogenesis in the developing vertebrate central nervous system. *Curr Opin Cell Biol* 17:648–657.
8. Farkas LM, Huttner WB (2008) The cell biology of neural stem and progenitor cells and its significance for their proliferation versus differentiation during mammalian brain development. *Curr Opin Cell Biol* 20:707–715.
9. Pontious A, Kowalczyk T, Englund C, Hevner RF (2008) Role of intermediate progenitor cells in cerebral cortex development. *Dev Neurosci* 30:24–32.
10. Miyata T, Kawaguchi D, Kawaguchi A, Gotoh Y (2010) Mechanisms that regulate the number of neurons during mouse neocortical development. *Curr Opin Neurobiol* 20:22–28.
11. Kriegstein AR, Götz M (2003) Radial glia diversity: A matter of cell fate. *Glia* 43:37–43.
12. Corbin JG, et al. (2008) Regulation of neural progenitor cell development in the nervous system. *J Neurochem* 106:2272–2287.
13. Kelava I, et al. (2012) Abundant occurrence of basal radial glia in the subventricular zone of embryonic neocortex of a lissencephalic primate, the common marmoset *Callithrix jacchus*. *Cereb Cortex* 22:469–481.
14. Smart IH, Dehay C, Giroud P, Berland M, Kennedy H (2002) Unique morphological features of the proliferative zones and postmitotic compartments of the neural epithelium giving rise to striate and extrastriate cortex in the monkey. *Cereb Cortex* 12:37–53.
15. Fish JL, Dehay C, Kennedy H, Huttner WB (2008) Making bigger brains-the evolution of neural-progenitor-cell division. *J Cell Sci* 121:2783–2793.
16. Noctor SC, Martínez-Cerdeño V, Ivic L, Kriegstein AR (2004) Cortical neurons arise in symmetric and asymmetric division zones and migrate through specific phases. *Nat Neurosci* 7:136–144.
17. Haubensak W, Attardo A, Denk W, Huttner WB (2004) Neurons arise in the basal neuroepithelium of the early mammalian telencephalon: A major site of neurogenesis. *Proc Natl Acad Sci USA* 101:3196–3201.
18. Miyata T, et al. (2004) Asymmetric production of surface-dividing and non-surface-dividing cortical progenitor cells. *Development* 131:3133–3145.
19. Attardo A, Calegari F, Haubensak W, Wilsch-Bräuninger M, Huttner WB (2008) Live imaging at the onset of cortical neurogenesis reveals differential appearance of the neuronal phenotype in apical versus basal progenitor progeny. *PLoS ONE* 3:e2388.
20. Shitamukai A, Konno D, Matsuzaki F (2011) Oblique radial glial divisions in the developing mouse neocortex induce self-renewing progenitors outside the germinal zone that resemble primate outer subventricular zone progenitors. *J Neurosci* 31: 3683–3695.
21. Wang X, Tsai JW, LaMonica B, Kriegstein AR (2011) A new subtype of progenitor cell in the mouse embryonic neocortex. *Nat Neurosci* 14:555–561.
22. Hansen DV, Lui JH, Parker PR, Kriegstein AR (2010) Neurogenic radial glia in the outer subventricular zone of human neocortex. *Nature* 464:554–561.
23. Fietz SA, et al. (2010) OSVZ progenitors of human and ferret neocortex are epithelial-like and expand by integrin signaling. *Nat Neurosci* 13:690–699.
24. Reillo I, de Juan Romero C, García-Cabezas MA, Borrell V (2011) A role for intermediate radial glia in the tangential expansion of the mammalian cerebral cortex. *Cereb Cortex* 21:1674–1694.
25. Wang WZ, Oeschger FM, Lee S, Molnár Z (2009) High quality RNA from multiple brain regions simultaneously acquired by laser capture microdissection. *BMC Mol Biol* 10:69.
26. Ayoub AE, et al. (2011) Transcriptional programs in transient embryonic zones of the cerebral cortex defined by high-resolution mRNA sequencing. *Proc Natl Acad Sci USA* 108:14950–14955.
27. Englund C, et al. (2005) Pax6, Tbr2, and Tbr1 are expressed sequentially by radial glia, intermediate progenitor cells, and postmitotic neurons in developing neocortex. *J Neurosci* 25:247–251.
28. Arai Y, et al. (2011) Neural stem and progenitor cells shorten S-phase on commitment to neuron production. *Nat Commun* 2:154.
29. Osumi N, Shinohara H, Numayama-Tsuruta K, Maekawa M (2008) Concise review: Pax6 transcription factor contributes to both embryonic and adult neurogenesis as a multifunctional regulator. *Stem Cells* 26:1663–1672.
30. Ochiai W, et al. (2009) Periventricular notch activation and asymmetric Ngn2 and Tbr2 expression in pair-generated neocortical daughter cells. *Mol Cell Neurosci* 40: 225–233.
31. Kowalczyk T, et al. (2009) Intermediate neuronal progenitors (basal progenitors) produce pyramidal-projection neurons for all layers of cerebral cortex. *Cereb Cortex* 19:2439–2450.
32. Woodruff RH, Tekki-Kessaris N, Stiles CD, Rowitch DH, Richardson WD (2001) Oligodendrocyte development in the spinal cord and telencephalon: Common themes and new perspectives. *Int J Dev Neurosci* 19:379–385.
33. Li H, Richardson WD (2008) The evolution of Olig genes and their roles in myelination. *Neuron Glia Biol* 4:129–135.
34. Huang da W, Sherman BT, Lempicki RA (2009) Systematic and integrative analysis of large gene lists using DAVID bioinformatics resources. *Nat Protoc* 4:44–57.
35. Lathia JD, et al. (2007) Patterns of laminins and integrins in the embryonic ventricular zone of the CNS. *J Comp Neurol* 505:630–643.
36. Lathia JD, Rao MS, Mattson MP, Ffrench-Constant C (2007) The microenvironment of the embryonic neural stem cell: lessons from adult niches? *Dev Dyn* 236:3267–3282.
37. Loulier K, et al. (2009) Beta1 integrin maintains integrity of the embryonic neocortical stem cell niche. *PLoS Biol* 7:e1000176.
38. Marthiens V, Kazanis I, Moss L, Long K, Ffrench-Constant C (2010) Adhesion molecules in the stem cell niche—More than just staying in shape? *J Cell Sci* 123:1613–1622.
39. Bradke F, Dotti CG (1998) Membrane traffic in polarized neurons. *Biochim Biophys Acta* 1404:245–258.
40. Ho Sui SJ, et al. (2005) oPOSSUM: Identification of over-represented transcription factor binding sites in co-expressed genes. *Nucleic Acids Res* 33:3154–3164.
41. Ho Sui SJ, Fulton DL, Arenillas DJ, Kwon AT, Wasserman WW (2007) oPOSSUM: Integrated tools for analysis of regulatory motif over-representation. *Nucleic Acids Res* 35(Web Server issue):W245–W252.
42. Kawaguchi A, et al. (2008) Single-cell gene profiling defines differential progenitor subclasses in mammalian neurogenesis. *Development* 135:3113–3124.
43. Johnson MB, et al. (2009) Functional and evolutionary insights into human brain development through global transcriptome analysis. *Neuron* 62:494–509.
44. Girós A, Morante J, Gil-Sanz C, Fairén A, Costell M (2007) Perlecan controls neurogenesis in the developing telencephalon. *BMC Dev Biol* 7:29.
45. Barros CS, Franco SJ, Müller U (2011) Extracellular matrix: Functions in the nervous system. *Cold Spring Harb Perspect Biol* 3:a005108.
46. Arikawa-Hirasawa E, et al. (2001) Dyssegmental dysplasia, Silverman-Handmaker type, is caused by functional null mutations of the perlecan gene. *Nat Genet* 27:431–434.
47. Hoyer J, Kraus C, Hammersen G, Geppert JP, Rauch A (2009) Lethal cutis laxa with contractural arachnodactyly, overgrowth and soft tissue bleeding due to a novel homozygous fibulin-4 gene mutation. *Clin Genet* 76:276–281.
48. Francis F, et al. (2006) Human disorders of cortical development: From past to present. *Eur J Neurosci* 23:877–893.
49. Javaherian A, Kriegstein A (2009) A stem cell niche for intermediate progenitor cells of the embryonic cortex. *Cereb Cortex* 19(Suppl 1):i70–i77.
50. Saito K, et al. (2009) Ablation of cholesterol biosynthesis in neural stem cells increases their VEGF expression and angiogenesis but causes neuron apoptosis. *Proc Natl Acad Sci USA* 106:8350–8355.
51. Stubbs D, et al. (2009) Neurovascular congruence during cerebral cortical development. *Cereb Cortex* 19(Suppl 1):i32–i41.